Current Applied Science and Technology e-ISSN: 2586-9396

Curr. Appl. Sci. Technol. 2026, Vol. 26 (No. 5), e0266010

Research article

Non-invasive Blood Glucose Measurement Using Near-infrared Spectroscopy and Microcontroller Equipment

Umpon Jairuk*, Akapong Phunpueok and Nithiwatthn Choosakul

Division of Physics, Faculty of Science and Technology, Rajamangala University of Technology Thanyaburi, Pathumthani, 12110, Thailand

Received: 20 January 2025, Revised: 21 July 2025, Accepted: 27 July 2025, Published: 1 December 2025

Abstract

This study focuses on the development of modern, non-invasive equipment for measuring blood glucose levels using near-infrared (NIR) spectroscopy with a transmitter of 940 nm wavelength light emitting diode (LED). The aim is to eliminate the need for invasive methods and provide greater convenience for patients. The equipment operates by emitting infrared spectrum from a high-speed LED VLSB3940, which is passed through the patient's fingertip and receive by a BPX 65 photodiode receiver. The received signal is converted into voltage by the BPX65 photodiode. The output voltage from the BPX65, which varies with glucose concentration in the blood, is then amplified by an operational amplifier (op-amp) circuit. The amplified voltages are collected by an Arduino microcontroller that is interfaced with a touch screen display. A corresponding C-Arduino language program controls all processes and displays the measurement results on the screen. The study concludes that the near-infrared spectrum can effectively transmit signals through the blood glucose in the fingertip, yielding results comparable to the old invasive method. The linear regression of invasive and non-invasive blood glucose measurements had R^2 values of 0.99 and 0.82, respectively. The plot of Clarke Error Grid Analysis (CEGA) showed that most of points were in zone A, indicating high accuracy. However, further development of the system is recommended, including the exploration of alternative transmitters of 1550 nm wavelength, better receivers, and circuits to optimize the equipment for commercial uses.

Keywords: non-invasive blood glucose; near-infrared spectroscopy; microcontroller

1. Introduction

Continuous blood glucose concentration (BGC) monitoring is an important strategy in the prevention of the development of diabetes in human. Diabetes is a health condition where the body either cannot use insulin effectively or does not produce enough of it, resulting in abnormal blood glucose levels. BGC can be measured in two different ways. Conventionally, invasive blood glucose monitor (IBGM) involves taking a tiny sample of blood with a finger prick, which is uncomfortable, and stopping blood collection to measure glucose

*Corresponding author: E-mail: umpon_j@rmutt.ac.th
https://doi.org/10.55003/cast.2025.266010
Copyright © 2025 by King Mongkut's Institute of Technology Ladkrabang, Thailand. This is an open access article under the CC BY-NC-ND license (http://creativecommons.org/licenses/by-nc-nd/4.0/).

concentration. This method can be quite expensive because the glucose strip is only used once, and it is unable to monitor blood sugar levels immediately when it is placed into a specific machine that runs on electricity. Alternatively, continuous glucose monitoring devices can be employed to track blood glucose levels continuously throughout the day (Olczuk & Priefer, 2018). Non-invasive blood glucose monitoring (NIBGM) is a preferable substitute. Numerous non-invasive techniques based on diverse technology are available for NIBGM. Another indirect way to assess blood sugar levels is with a breathalyzer, which measures the quantity of acetone in the breath. Various techniques employ finger detection as a non-invasive means of measurement. As an illustration, metabolic heat conformation (MHC) measurement and heat release measurement are used to track glucose levels (Tang et al., 2008). MHC involves the measurement of the heat produced when the body burns sugar to produce energy. Heat is produced when glucose is utilized as fuel. When oxygen and glucose are delivered to cells through blood arteries, the body creates heat (Cho et al., 2004).

The type of light used in near-infrared spectroscopy (NIR) has wavelengths ranging from 780 to 2500 nm (Zhang et al., 2019). Research on this strategy is still ongoing such as a non-contact method of measuring blood glucose levels in the body by using mid-infrared spectroscopy to examine the epidermis immediately. Between less than 50 mg/dL and more than 300 mg/dL of sugar can be found in the skin. For those who have diabetes, it is crucial to monitor this range (Pleitez et al., 2012). Because human bodies emit mid-infrared radiation, which varies depending on blood sugar levels, it is possible to assess blood sugar levels using MIRS methods (Yeh et al., 2014). The speed of sound that passes through tissues is used in ultrasonic technologies (Harman-Boehm et al., 2010; Srivastava et al., 2014). There is a theory that links the body's glucose levels to the speed of sound. Elevated blood sugar causes sound waves to move through the body more quickly. As a result of this, they may travel in less time. The methods widely used are non-invasive optical glucose monitoring by using near-infrared (NIR) or mid infrared (MIR) spectrum passing through fingertip, and then measuring output voltage of receiver. However, using voltage amplifier for simplicity on displaying is needed.

A set of electronical devices, that are easy to obtain and cheap and include a signal voltage amplifier circuit for non-invasive blood glucose testing using the 940 nm near-infrared (NIR) spectrum, is used in this research. The devices include an LED transmitter, a BPX 65 photodiode receiver, and a touch screen display that attaches to an Arduino microcontroller, which collects voltages. The measurement results are shown on the screen via a corresponding C-Arduino language software, which also manages all operations. The glucose molecule has a unique absorption pattern at 940 nm, which is in the NIR band, and 940 nm is the target wavelength. The developed system was put into practice at the user's fingertips to obtain data quickly and easily without requiring any intervention or discomfort to the body. A linear graph of blood glucose concentration vs voltage is plotted using the voltage data that has been gathered.

2. Materials and Methods

Blood circulates widely in the human body, and plasma which is liquid composed primarily of water, makes up most of the blood. Other components, such as proteins, minerals, and lipids make up the remaining plasma (Zirk & Poetzschke, 2004). Blood includes 40% red blood cells and fewer than 1% of white blood cells and platelets in addition to the liquid portion (Dean, 2005). Through tiny blood arteries, the sugar in the liquid portion of the blood is converted to energy that can be utilized immediately or stored for later. Sugar enters the fluid surrounding the cells in the tiny blood vessels. Small veins known as venules carry

blood from capillaries, or tiny blood arteries, back to the heart. The blood is then returned to the heart via larger veins. The blood sugar content in the arteries and small blood vessels is nearly identical (Cengiz & Tamborlane, 2009). Insulin and glucagon regulate the amount of ketones in a healthy body. These hormones aid in regulating the production of ketones. Patients with diabetes who do not get enough insulin may have blood ketones that are excessively high. Consequently, in cases where the body experiences diabetic ketoacidosis (DKA) (Laffel, 1999), then an excessive level of ketones in the blood can make it overly acidic, which can put a person in a coma or even kill them if treatment is not received (Umpierrez & Korytkowski, 2016).

One method of measuring blood glucose is the non-invasive blood glucose measurement approach, which makes use of the intrinsic properties of glucose. The goal of this research was to create a non-invasive blood glucose level testing tool that measured blood glucose concentration by utilizing the near-infrared spectrum as a source. Less test strips are needed for each measurement with this pleasant procedure. Because it is non-invasive, the general population can readily use and promote it to monitor their daily health, allowing for changes in their food or exercise routines to achieve optimal health. Glucose molecules have a high absorbance efficiency for light of 940 nm, which is in the near-infrared light. Furthermore, compared to near-infrared and red-light spectra, it is discovered that the majority of biological cells and tissues exhibit remarkable transparency in the 700-1100 nm wavelength region. Most of appropriate wavelengths for glucose level detection are 780 and 940 nm, the spectrum over 1000 nm is less responsible because the spectrum may be absorbed by water.

2.1 Scattering and occlusion spectroscopy

The spectrum of the scattering of NIR light after passing through a tissue sample depends on several parameters, such as the reduced scattering coefficient of tissue (μ_s') which depends on the mismatch between the refractive index of the extracellular fluid and the refractive index of the tissue membranes and cellular components (Larin et al., 2002). The behavior of reduced scattering coefficient of tissue (μ_s') as a function of refractive index of the extracellular fluid (n_m) and the refractive index of cellular membrane (n_s) is shown in equation (1) (Larin et al., 2003).

$$\mu_s' = 3.28\pi r^2 \rho_s \left(\frac{2\pi r}{\lambda}\right)^{0.37} \left(\frac{n_s - n_m}{n_m}\right)^{2.09} \quad (1)$$

where r_s is the radius of scattering sphere, ρ_s is the volume of density spheres and λ is the wavelength of incident light, respectively. Refractive index of the extracellular fluid (n_m) is not constant, in which increasing by 1.52 x 10^{-5} can cause 10 mg/dl increasing in glucose concentration (Mishchenko, 2009; Zhou et al., 2011). However, the refractive index of cellular membrane (n_s) is constant (Maier, 1994). Figure 1 showed that the scattering angle θ_a of low glucose concentration sample exceeds that θ_b of the high glucose concentration sample, and thus the intensity of the scattered light at the detector for the low concentration sample is less than that of the high glucose concentration sample.

The energy of the incident light and the scattered light are the same in elastic scattering. On the other hand, inelastic scattering results in scattered light with less energy than incident light (Boustany, 2010; Madsen, 2016). The energy of the incident light and the structure of the material both affect the direction or angle of dispersed light. When light interacts with tissue, it might scatter forward in a single scattering event or deviate in many scattering events within the tissue as shown in Figure 2.

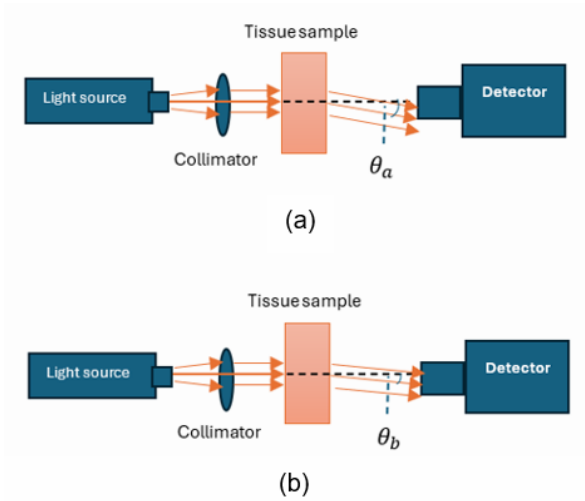

Figure 1. Schematic of scattering spectroscopy of a (a) low concentration of glucose sample $C_a < C_a \rightarrow (\mu_s)_a > (\mu_s)_b \rightarrow I_a < I_b \,\&\, \theta_a > \theta_b$
(b) high concentration of glucose sample

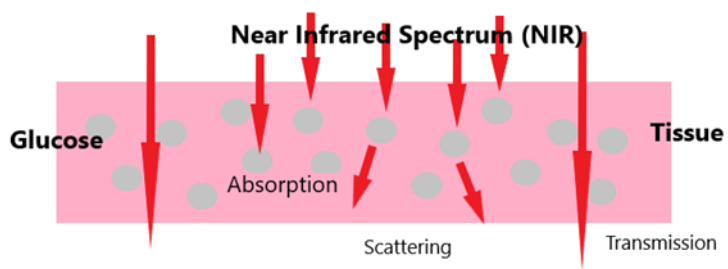

Figure 2. Interactions of near infrared spectrum (NIR) and tissue

2.2 Beer-Lambert law

Analytical spectroscopy uses the Beer-Lambert Law, which states that the amount of energy absorbed or transmitted by a solution is exactly proportional to the concentration of the solute and the molar absorptivity of the solution, to quantify the absorbance of different samples. This law is also known by the names Beer's Law and Lambert's Law, which provide a thorough grasp of how a substance attenuates light and its associated qualities as shown in Figure 3.

A derivation of the Beer-Lambert law lead to equation (2), where I_0(W/cm^2) is the initial intensity, I is the intensity of light in W/cm^2, l is the absorption depth of sample in cm, c is the concentration of absorbing molecules in mmol/L, ε is the molar extinction coefficient or molar attenuation coefficient in L (mmol·cm), α is the absorption coefficient. T is the transmittance, and A is the absorbance of sample according to equations (3) and (4), respectively (Swinehart, 1962).

$$I = I_0 e^{-\alpha l} \tag{2}$$

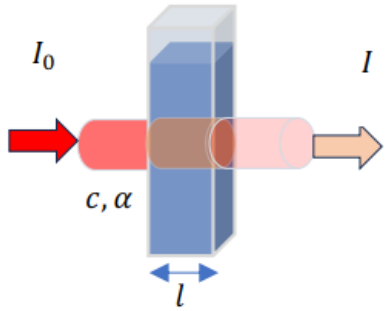

Figure 3. Beer-Lambert's law, absorption of light by solution

$$T = \frac{I}{I_0} = e^{-\alpha l} \tag{3}$$

$$A = log\left(\frac{1}{T}\right) = log\left(\frac{I_0}{I}\right) = \alpha l = \varepsilon c l \tag{4}$$

The accuracy of measurement by the invasive blood glucose method may be effected from the components as interferers while measuring blood glucose. To minimize the absorption due to all unwanted components, the wavelength of the light source should be highly absorbed by glucose but non-interactive with blood and tissue components. Potential absorbing tissue components include melanin (hair and skin human color), beta-carotene (yellow color of tissues) and fatty tissues (which vary in different individuals). The absorbing blood components such as albumin (3.5-5 g/dL), globulin (2.5-3 g/dL) and hemoglobin (11.5-13.7 g/dL) are generally at much higher concentrations than glucose (0.065-0.105 g/dL), so their contribution to light absorption can be significant (Busher, 1990; Beutler & Waalen, 2006; Shaw & Mantsch, 2006; Wood et al., 2008).

2.3 Theoretical background

There are several non-invasive glucose sensing methods that can be utilized, and the methods rely on the intrinsic properties of glucose. Absorption and scattering in the near-infrared (NIR) and mid-infrared (MIR) wavelength ranges of 2500-25,000 nm and 700-2,500 nm, respectively, are utilized and examples include the absorption of IR by glucose in water (Shaw & Mantsch, 2006; Oliver et al., 2009; So et al., 2012). Water absorbs light in two peaks between 1,350 and 1,520 nm and 1,790 and 2,000 nm in the near-infrared (Kozma, 2014). In the near-infrared (NIR) region, glucose absorbs in three peaks: 700-1,100 nm, 1,500-1,850 nm, and 2,000-2,400 nm (Haaland et al., 1992; Yadav et al., 2014; Maruo & Yamada, 2015). In comparison to shorter ranges (1,500-1,850 nm and 700-1,100 nm), glucose absorbs light more efficiently in the 2,000-2,400 nm range, while water exhibits weaker light absorption in these shorter ranges. Multiple absorption peaks may be seen in the absorbance spectra of glucose in the MIR range of 6,250-11,110 nm, especially between 8,696 and 10,000 nm (McNichols & Coté, 2000). In comparison, water exhibits significantly higher light absorption in the MIR region than the NIR range. The amount of light absorbed is largely dependent on how much of it is absorbed by tissue and blood components. A cumulative measure of all the absorbing entities' absorption coefficients is called the absorption coefficient (Jacques, 2013).

The wavelength of light source should be chosen for maximal absorption by glucose and minimum absorption by other blood and tissue components in order to reduce absorption by non-target components. For glucose, protein, fat, and water, Maruo and Yamada (2015) measured absorption maxima at 1,600, 1,510, 1,727, and 1,450 nm, respectively, in the near-infrared (NIR) region between 1,300 and 1,900 nm. Likewise, Kasahara et al. (2017) detected three absorption peaks at 1,036, 1,080, and 1,110 cm^{-1} in the MIR range between 900-1,200 cm^{-1} for a 1% glucose solution.

Multiple tissue components display scattering and deviation from the Beer-Lambert law and the equation $I=I_0\exp(-(\alpha+\alpha_s\ (1-\cos\delta))l)$, δ=scattering angle. The scattering coefficient, α_s, is used to account for the deviations (Rogers et al., 2013).

In polarimetry, the rotation of the electric field's angle is measured as light passes through an optically active solution, like glucose in solution, using linearly polarized light. Figure 4 comprises a polarimeter with components such a light source, linear polarizer, sample, polarization analyzer, and photodetector.

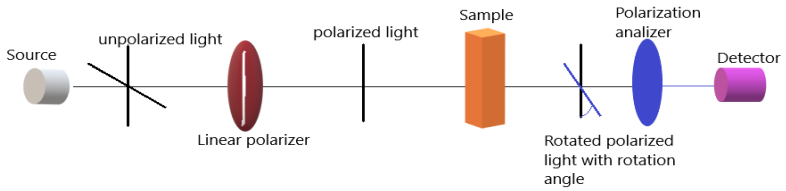

Figure 4. Simplified schematic polarimeter

The rotation angle of the electric field depends on the glucose concentration in the optically active aqueous solution, as described by equation (5) (Al-Hafidh et al., 2019):

$$\theta = \alpha_\lambda^T\ lc\ , \tag{5}$$

where θ is the angle of rotation of the electric field, α_λ^T is the specific rotation for an active substance in (mL)/(dm g), l is the optical path length within the active aqueous solution (dm), and c is the concentration of the active substance (g/mL). The value of the specific rotation, α_λ^T, for an active molecule depends on the wavelength of the light source and the temperature of the sample. The electric field's angle of rotation shifts clockwise when light passes through a glucose solution sample.

One of difficulties for glucose sensing in biological tissue is multiple light scattering, which results in changes in polarization vector orientation and depolarization of light. Thus, glucose concentration within the tissue cannot be measured accurately. A possible method to measure glucose in scattering media is provided by a Mueller matrix polarimetry system, which can extract the optical rotation angle and depolarization properties of a sample (Mukherjee et al., 2018; Al-Hafidh et al., 2019).

2.4 Equipment and assembly

A block diagram of the devices can be design as shown in Figure 5. Figure 6(a) shows the circuit of transmitter-receiver and operational-amplifier, which can be interfaced with the Arduino mega 2560 ADK board, shield board and display board (Figure 6(b)).

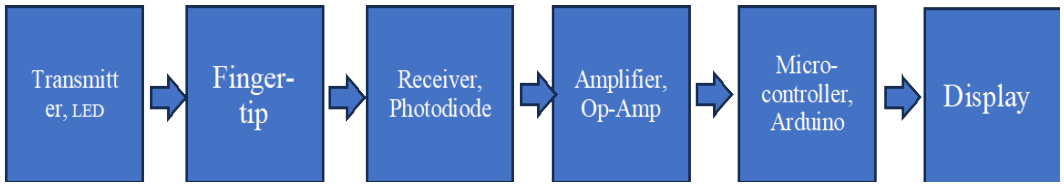

Figure 5. Block diagram of the devices

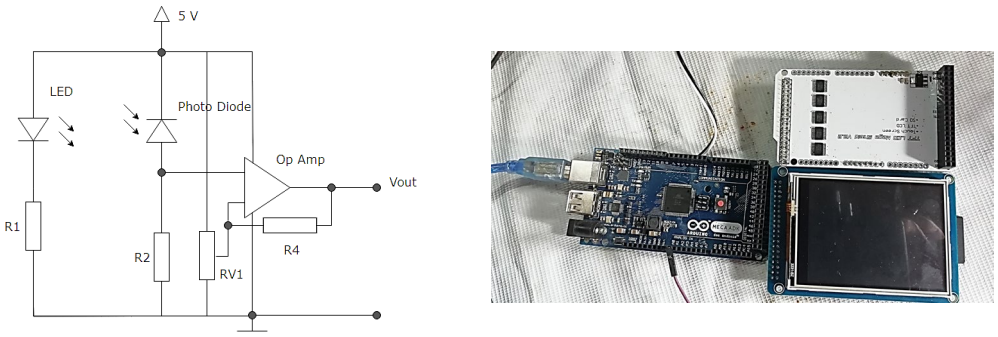

(a) (b)

Figure 6. (a) The circuit of transmitter-receiver and operational-amplifier, (b) Arduino mega 2560 ADK board, shield-board and display board

The first step in the preparation process involves using a protoboard to connect all of the devices simply, as shown in Figure 7(a). Next, we adjusted the values of some variable resistors to make the circuit work properly. Finally, we tested the circuit's functionality. For convenience and standardization, we also constructed the circuit on a PCB protoboard, as illustrated in Figure 7(b). The shield board and display board for the Arduino Mega 2560 ADK microcontroller board were constructed as seen in Figure 8(a), with Figure 8(b) showing the top view of the assembled boards. The program that read the control data and displayed the blood glucose level output had to be coded. After assembling all of the components and placing them in the box, the system was powered by a 5-volt power storage device. For easy measurement, the transmitter and receiver were held in place using the fingertip clamp, as seen in Figures 9(a) and (b).

(a) (b)

Figure 7. (a) Preparation for measuring output voltage vs. glucose concentration on protoboard, (b) all devices from protoboard building on PCB protoboard

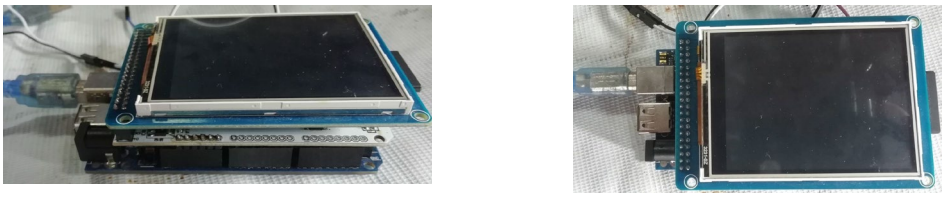

(a) (b)

Figure 8. (a) Assembling of Arduino mega 2560 ADK board, shield board and display board, (b) top view of assembled boards

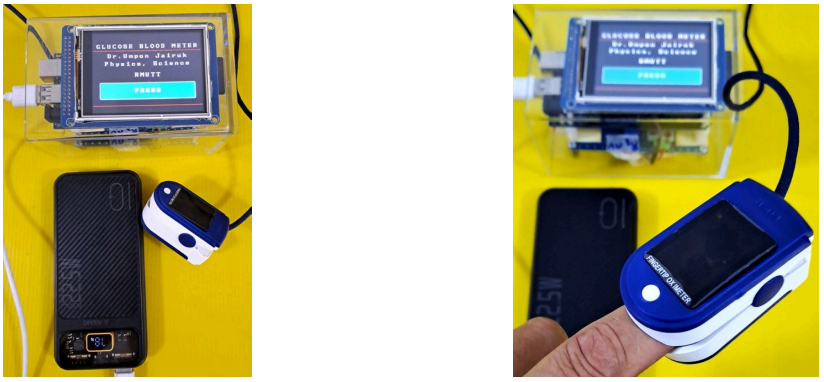

(a) (b)

Figure 9. (a) Complete set of “Glucose Blood Meter”, (b) showing measurement

3. Results and Discussion

As illustrated in Figures 9(a) and (b), we modified the output voltage once the transmitter-receiver and amplifier board were constructed. Next, using water for injection, we diluted the 50% glucose for medical grade (10 mL). We made concentrations of 83.3, 100, 125, 142.9, and 166.7 mg/dl as shown in Table 1.

Once the diluted glucose was placed within the cuvette, the findings were displayed in Table 2. The cuvette was then exposed to NIR light from an LED at 940 nm, which measured the relationship between the output voltage (V) and the concentration of glucose (mg/dl). The graph in Figure 10 displays the linear equation representing the relationship between the output voltage trend and glucose concentration according to equation (6):

$$0.0125C - 0.2706, R^2 = 0.9963 \quad (6)$$

where V_o is output voltage (V) and C is the concentration. When the "Blood Glucose Meter" was complete, it was used to measure the blood glucose levels of ten individuals, as indicated in Table 2. The industry standard is AccuCheck Instant, which requires a

Table 1. Preparation of the glucose concentration(mg/mL)

Add Injecting Water(V) (mL)	Mass/(10+V) (mg/mL)	Glucose Intensity (mg/mL)
100	5,000/(10+100)	45.5
90	5,000/(10+90)	50.0
80	5,000/(10+80)	55.6
70	5,000/(10+70)	62.5
60	5,000/(10+60)	71.4
50	5,000/(10+50)	83.3
40	5,000/(10+40)	100
30	5,000/(10+30)	125
20	5,000/(10+20)	142.9
10	5,000/(10+10)	166.7

Table 2. The glucose concentration(mg/mL) vs. output voltage (V) of the amplified device (op-amp)

Glucose Concentration (mg/mL)	Output Voltage (V)
45.5	0.28
50.0	0.36
55.6	0.45
62.5	0.52
71.4	0.64
83.3	0.75
100	0.96
125	1.22
142.9	1.56
166.7	1.82

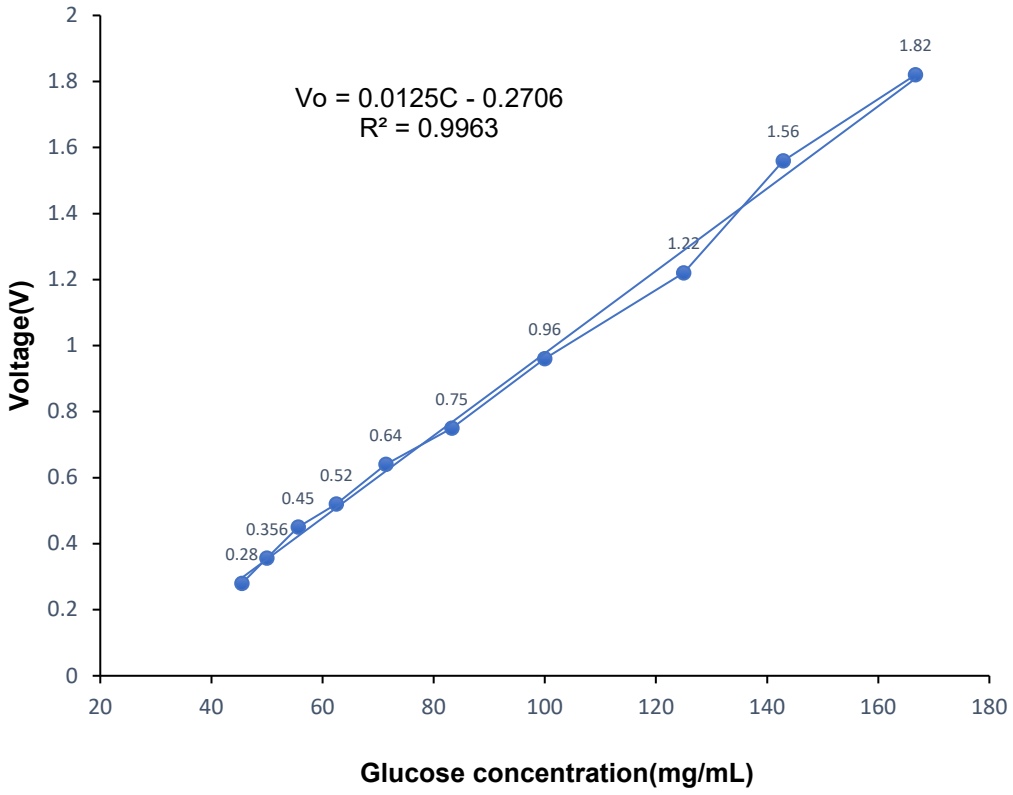

Figure 10. The plot of the relation of glucose concentration vs. output voltage

particular type of strip to measure blood sugar. Initially, the 25 participants in Table 3 took their weight and height, took a picture of their forefinger, and completed an informedconsent form which included questions about their age and willingness to be tested and assessed. AccuCheck Instant was then used to measure the subjects' blood glucose levels. The user used our device for five seconds on each of the thumb after the result was achieved. The results were compared to the invasive blood glucose level value. The blood glucose concentration plotting graph, displayed in Figure 11, was the final step. The root mean square error (RMSE) of the traditional invasive and average non-invasive blood glucose level detection data were 0.9914 and 09951, respectively.

Table 3 shows the data from the invasive blood glucose level measurement and non-invasive blood glucose measurement. We then plotted the graph by using Clarke error grid analysis by plotting the reference glucose concentrations and the glucose monitor glucose concentrations. Considering the points in zone A-E of the graph, we found that most of points were in zone A or B of the graph, as shown in Figure 12.

Table 3. Comparing the values of the invasive blood glucose measurement and non-invasive blood glucose measurement

Number	Reference Glucose (mg/dl)	Glucose Monitor Glucose (mg/dl)	% Error
1	76	74.30	-2.24
2	81	74.60	-7.90
3	86	100.20	16.51
4	88	93.25	5.97
5	90	92.40	2.67
6	96	94.23	-1.84
7	98	117.24	19.63
8	101	102.60	1.58
9	105	110.82	5.54
10	108	115.36	6.81
11	110	84.81	-22.90
12	112	122.25	9.15
13	119	130.50	9.66
14	123	118.25	-3.86
15	126	138.40	9.84
16	130	136.22	4.78
17	132	145.22	10.02
18	135	146.40	8.44
19	140	144.20	3.00
20	146	135.80	-6.99
21	150	153.20	2.13
22	158	147.80	-6.46
23	161	145.40	-9.69
24	166	130.40	-21.45
25	170	160.60	-5.53

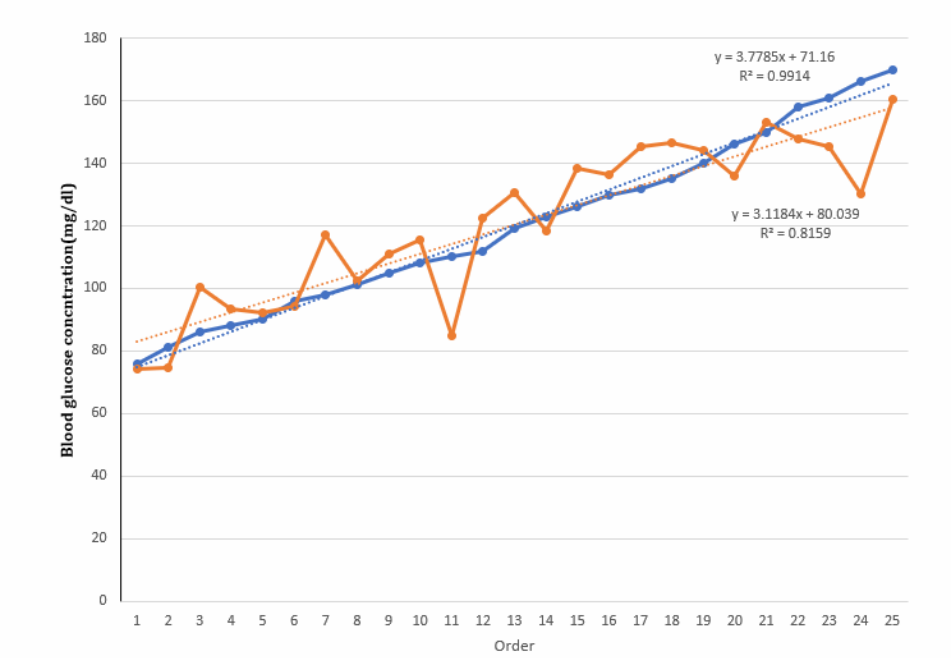

Figure 11. Comparison of blood glucose concentration in case of invasive blood glucose measurement and non-invasive blood glucose measurement

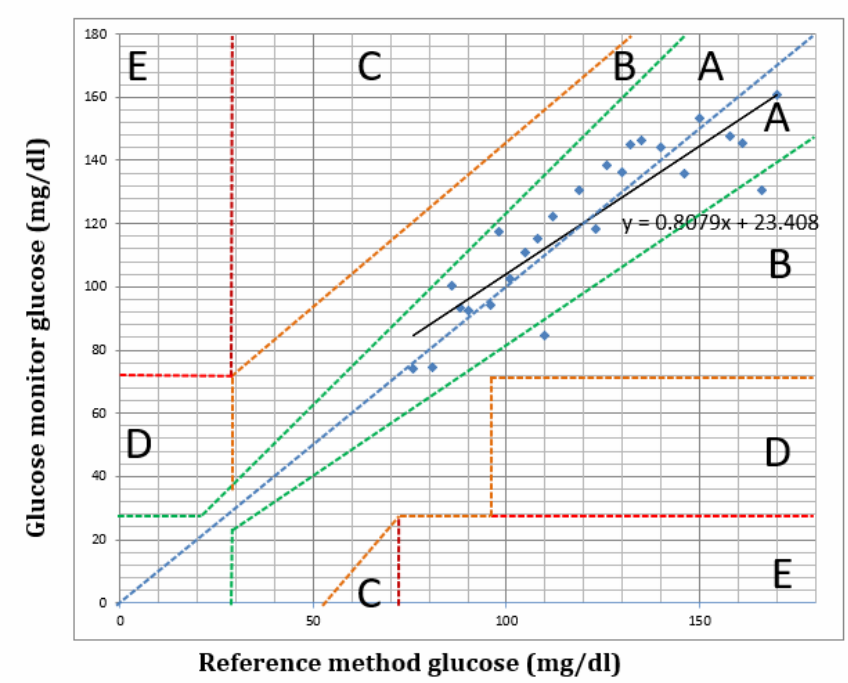

Figure 12. Plot of Clarke Error Grid Analysis

4. Conclusions

The relation between voltages and concentration of glucose solution expressed as a linear equation is shown in equation (6), with R^2=0.9963, and graphically in Figure 9. Figure 10, which shows that blood glucose concentrations in case of invasive blood glucose measurement and non-invasive blood glucose measurement had root mean square errors (RMSE) of 0.9914 and 0.8159, respectively. This indicates that the measurements obtained using conventional invasive and non-invasive techniques were correct. Moreover, the Clarke Error Grid Analysis plot showed that most points fell in zones A and B, which were the zones of high accuracy.

However, the blood glucose meter can be improved by using a transmitter that operates in the NIR band and produces a wavelength higher than 940 nm. For example, the 1550 nm region corresponds to second overtone absorption of the O–H bond in glucose, which enables more specific molecular targeting and by changing the receiver to a higher accuracy receiver, such as the FGA10. Additionally, the advancement of microcontrollers allows for the convenient usage of small displays. Furthermore, the limitations of the study should be clearly acknowledged, including factors such as potential interference from other biological molecules and changes in tissue properties.

5. Acknowledgements

The researchers are grateful to the “Research Promotion Fund for new generation researchers”, Rajamangala University of Technology Thanyaburi. And thanks to Asst. Prof. Dr. Prasopchai Viriyasrisuwattana, for guiding and advising in electronics parts in this research.

6. Authors’ Contributions

Umpon Jairuk: Writing – original draft, Conceptualization, Formal analysis, Investigation, Funding acquisition. Akapong Phunpueok: Writing – review & editing, Resources, Investigation, Formal analysis, Supervision. Nithiwatthn Choosakul: Writing – original draft, Data curation, Investigation, Formal analysis.

ORCID

Umpon Jairuk https://orcid.org/0000-0003-1101-2077

Akapong Phunpueok https://orcid.org/0000-0002-9745-3457

Nithiwatthn Choosakul https://orcid.org/0009-0009-0023-6957

7. Conflicts of Interest

The authors declare that they have no conflicts of interest.

References

Al-Hafidh, M. H., Glidle, A., Wilson, R., Kelly, A. E., Reboud, J., & Cooper, J. M. (2019). Multireflection polarimetry in microfluidics. *IEEE Sensors Letters*, *3*(10), 1-4. https://doi.org/10.1109/lsens.2019.2943688

Beutler, E., & Waalen, J. (2006). The definition of anemia: what is the lower limit of normal of the blood hemoglobin concentration? *Blood*, *107*(5), 1747-1750. https://doi.org/10.1182/blood-2005-07-3046

Boustany, N. N., Boppart, S. A., & Backman, V. (2010). Microscopic imaging and spectroscopy with scattered light. *Annual Review of Biomedical Engineering*, *12*(1), 285-314. https://doi.org/10.1146/annurev-bioeng-061008-124811

Busher, J. T. (1990) Serum albumin and globulin. In H. K. Walker, W. D. Hall, & J. W. Hurst (Eds.). *Clinical methods: The history, physical, and laboratory examinations* (3rd Ed., pp. 497-499). Butterworths. https://www.ncbi.nlm.nih.gov/books/NBK204/

Cengiz, E., & Tamborlane, W. V. (2009). A tale of two compartments: interstitial versus blood glucose monitoring. *Diabetes Technology and Therapeutics*, *11*(S1), S-11-S-16. https://doi.org/10.1089/dia.2009.0002

Cho, O. K., Kim, Y. O., Mitsumaki, H., & Kuwa, K. (2004). Noninvasive Measurement of Glucose by Metabolic Heat Conformation Method. *Clinical Chemistry*, *50*(10), 1894-1898. https://doi.org/10.1373/clinchem.2004.036954

Dean, L. (2005). *Hemolytic disease of the newborn*. National Center for Biotechnology Information (US). https://www.ncbi.nlm.nih.gov/books/NBK2266/

Haaland, D. M., Robinson, M. R., Koepp, G. W., Thomas, E. V., & Eaton, R. P. (1992). Reagentless near-infrared determination of glucose in whole blood using multivariate calibration. *Applied Spectroscopy*, *46*(10), 1575-1578. https://doi.org/10.1366/000370292789619232

Harman-Boehm, I., Gal, A., Raykhman, A. M., Naidis, E., & Mayzel, Y. (2010). Noninvasive glucose monitoring: Increasing accuracy by combination of multi-technology and multi-sensors. *Journal of Diabetes Science and Technology*, *4*(3), 583-595. https://doi.org/10.1177/193229681000400312

Jacques, S. L. (2013). Optical properties of biological tissues: a review. *Physics in Medicine and Biology*, *58*(11), R37-R61. https://doi.org/10.1088/0031-9155/58/11/r37

Kasahara, R., Kino, S., Soyama, S., & Matsuura, Y. (2017). Noninvasive glucose monitoring using mid-infrared absorption spectroscopy based on a few wavenumbers. *Biomedical Optics Express*, *9*(1), Article 289. https://doi.org/10.1364/boe.9.000289

Kozma, B., Párta, L., Zalai, D., Gergely, S., & Salgó, A. (2014). A model system and chemometrics to develop near infrared spectroscopic monitoring for Chinese hamster ovary cell cultivations. *Journal of Near Infrared Spectroscopy*, *22*(6), 401-410. https://doi.org/10.1255/jnirs.1133

Laffel, L. (1999). Ketone bodies: a review of physiology, pathophysiology and application of monitoring to diabetes. *Diabetes/Metabolism Research and Reviews*, *15*(6), 412-426. https://doi.org/10.1002/(sici)1520-7560(199911/12)15:6%3C412::aid-dmrr72%3E3.0.co;2-8

Larin, K. V., Eledrisi, M. S., Motamedi, M., & Esenaliev, R. O. (2002). Noninvasive blood glucose monitoring with optical coherence tomography: A pilot study in human subjects. *Diabetes Care*, *25*(12), 2263-2267. https://doi.org/10.2337/diacare.25.12.2263

Larin, K. V., Motamedi, M., Ashitkov, T. V., & Esenaliev, R. O. (2003). Specificity of noninvasive blood glucose sensing using optical coherence tomography technique: a pilot study. *Physics in Medicine and Biology*, *48*(10), 1371-1390. https://doi.org/10.1088/0031-9155/48/10/310

Madsen, S. J. (2016). Physics of photodynamic therapy. In B. J.-F. Wong, & J. Ilgner (Eds.). *Biomedical Optics in Otorhinolaryngology* (pp. 287-309). Springer. https://doi.org/10.1007/978-1-4939-1758-7_18

Maier, J. S., Walker, S. A., Fantini, S., Franceschini, M. A., & Gratton, E. (1994). Possible correlation between blood glucose concentration and the reduced scattering coefficient of tissues in the near infrared. *Optics Letters*, *19*(24), 2062-2064. https://doi.org/10.1364/ol.19.002062

Maruo, K., & Yamada, Y. (2015). Near-infrared noninvasive blood glucose prediction without using multivariate analyses: introduction of imaginary spectra due to scattering change in the skin. *Journal of Biomedical Optics*, *20*(4), Article 047003. https://doi.org/10.1117/1.jbo.20.4.047003

McNichols, R. J., & Coté, G. L. (2000). Optical glucose sensing in biological fluids: an overview. *Journal of Biomedical Optics*, *5*(1), 5-16. https://doi.org/10.1117/1.429962

Mishchenko, M. I. (2009). Tissue optics: Light scattering methods and instruments for medical diagnostics, V. Tuchin. 2nd ed. SPIE Press, Bellingham, WA (2007) Hardbound, ISBN 0-8194-6433-3, xl+841pp. *Journal of Quantitative Spectroscopy and Radiative Transfer*, *110*(8), 528. https://doi.org/10.1016/j.jqsrt.2009.02.009

Mukherjee, P., Hagen, N., & Otani, Y. (2018). Glucose sensing in the presence of scattering by analyzing a partial Mueller matrix. *Optik*, *180*, 775-781. https://doi.org/10.1016/j.ijleo.2018.11.157

Olczuk, D., & Priefer, R. (2018). A history of continuous glucose monitors (CGMs) in self-monitoring of diabetes mellitus. *Diabetes and Metabolic Syndrome, 12*(2), 181-187. https://doi.org/10.1016/j.dsx.2017.09.005

Oliver, N. S., Toumazou, C., Cass, A. E. G., & Johnston, D. G. (2009). Glucose sensors: a review of current and emerging technology. *Diabetic Medicine*, *26*(3), 197-210. https://doi.org/10.1111/j.1464-5491.2008.02642.x

Pleitez, M. A., Lieblein, T., Bauer, A., Hertzberg, O., von Lilienfeld-Toal, H., & Mäntele, W. (2012). *In vivo* noninvasive monitoring of glucose concentration in human epidermis by mid-infrared pulsed photoacoustic spectroscopy. *Analytical Chemistry*, *85*(2), 1013-1020. https://doi.org/10.1021/ac302841f

Rogers, J. D., Radosevich, A. J., Yi, J., & Backman, V. (2013). Modeling light scattering in tissue as continuous random media using a versatile refractive index correlation function. *IEEE Journal of Selected Topics in Quantum Electronics*, *20*(2), Article 7000514. https://doi.org/10.1109/jstqe.2013.2280999

Shaw, R. A., & Mantsch, H. H. (2006). Infrared spectroscopy in clinical and diagnostic analysis. *Encyclopedia of Analytical Chemistry*. John Wiley & Sons. https://doi.org/10.1002/9780470027318.a0106

So, C.-H., Choi, K.-S., Wong, T. K., & Chung, J. W. (2012). Recent advances in noninvasive glucose monitoring. *Medical Devices*, *5*, 45-52. https://doi.org/10.2147/mder.s28134

Srivastava, A., Chowdhury, M. K., Sharma, S., & Sharma, N. (2014). Measurement of glucose by using modulating ultrasound with optical technique in normal and diabetic human blood serum. In *2014 International conference on advances in engineering and technology research* (pp. 1-5). IEEE. https://doi.org/10.1109/ICAETR.2014.7012942

Swinehart, D. F. (1962). The Beer-Lambert law. *Journal of Chemical Education*, *39*(7), Article 333. https://doi.org/10.1021/ed039p333

Tang, F., Wang, X., Wang, D., & Li, J. (2008). Non-Invasive glucose measurement by use of metabolic heat conformation method. *Sensors*, 8(5), 3335-3344. https://doi.org/10.3390/s8053335

Umpierrez, G., & Korytkowski, M. (2016). Diabetic emergencies - ketoacidosis, hyperglycaemic hyperosmolar state and hypoglycaemia. *Nature Reviews. Endocrinology*, *12*(4), 222-232. https://doi.org/10.1038/nrendo.2016.15

Wood, M. F. G., Côté, D., & Vitkin, I. A. (2008). Combined optical intensity and polarization methodology for analyte concentration determination in simulated optically clear and turbid biological media. *Journal of Biomedical Optics*, *13*(4), Article 044037. https://doi.org/10.1117/1.2968198

Yadav, J., Rani, A., Singh, V., & Murari, B. M. (2014). Near-infrared LED based non-invasive blood glucose sensor. In *International conference on signal processing and integrated networks (SPIN)* (pp. 591-594). IEEE. https://doi.org/10.1109/SPIN.2014.6777023

Yeh, Y.-C., Yang, S., Zhao, F., & Schmidt, D. (2014). Noninvasive glucose monitoring by mid-infrared self-emission method. In *Proceedings of the international joint conference on biomedical engineering systems and technologies* (pp. 107-111). Science and Technology Publications. https://doi.org/10.5220/0004750101070111

Zhang, R., Liu, S., Jin, H., Luo, Y., Zheng, Z., Gao, F., & Zheng, Y. (2019). Noninvasive electromagnetic wave sensing of glucose. *Sensors*, *19*(5), Article 1151. https://doi.org/10.3390/s19051151

Zhou, Y., Zeng, N., Ji, Y., Li, Y., Dai, X., Li, P., Duan, L., Ma, H., & He, Y. (2011). Iris as a reflector for differential absorption low-coherence interferometry to measure glucose level in the anterior chamber. *Journal of Biomedical Optics*, *16*(1), Article 015004. https://doi.org/10.1117/1.3528658

Zirk, K., & Poetzschke, H. (2004). On the suitability of refractometry for the analysis of glucose in blood-derived fluids. *Medical Engineering and Physics*, *26*(6), 473-481. https://doi.org/10.1016/j.medengphy.2004.03.008